

# Quetiapine induces myocardial necroptotic cell death through bidirectional regulation of cannabinoid receptors

Xiaoqing Li<sup>a</sup>, Zhao Peng<sup>a</sup>, Yiling Zhou<sup>a</sup>, Jing Wang<sup>a</sup>, Xinyi Lin<sup>a</sup>, Xiaoru Dong<sup>a</sup>, Xiaochen Liu<sup>a</sup>, Jieqing Jiang<sup>a</sup>, Yan Jiang<sup>a,\*</sup>, Liliang Li<sup>a,b,\*</sup>

<sup>a</sup> Department of Forensic Medicine, School of Basic Medical Sciences, Fudan University, Shanghai, 200032, China

<sup>b</sup> Shanghai Key Laboratory of Crime Scene Evidence, Shanghai Public Security Bureau, Shanghai 200083, China

## ARTICLE INFO

### Keywords:

Antipsychotics  
Quetiapine  
Endocannabinoid system  
Necroptosis  
Cardiotoxicity

## ABSTRACT

Quetiapine is a common atypical antipsychotic used to treat mental disorders such as schizophrenia, bipolar disorder, and major depressive disorder. There has been increasing number of reports describing its cardiotoxicity. However, the molecular mechanisms underlying quetiapine-induced myocardial injury remain largely unknown. Herein, we reported a novel cell death type, quetiapine-induced necroptosis, which accounted for quetiapine cardiotoxicity in mice and proposed novel therapeutic strategies. Quetiapine-treated hearts showed inflammatory infiltration and evident fibrosis after 21-day continuous injection. The specific increases of protein levels of RIP3, MLKL and the phosphorylation of MLKL showed that quetiapine induced necroptotic cell death both *in vivo* and *in vitro*. Pharmacologic blockade of necroptosis using its specific inhibitor Necrostatin-1 attenuated quetiapine-induced myocardial injury in mice. In addition, quetiapine imbalanced the endocannabinoid system and caused opposing effects on two cannabinoid receptors (CB1R and CB2R). Specific antagonists of CB1R (AM 281, Rimonabant), but not its agonist ACEA significantly ameliorated the heart histopathology induced by chronic quetiapine exposure. By contrast, specific agonists of CB2R (JWH-133, AM 1241), but not its antagonist AM 630 exerted beneficial roles against quetiapine cardiotoxicity. The protective agents (AM 281, Rimonabant, AM 1241, and JWH-133) consistently inactivated the quetiapine-induced necroptosis signaling. Quetiapine bidirectionally regulates cannabinoid receptors and induces myocardial necroptosis, leading to cardiac toxic effects. Therefore, pharmacologic inhibition of CB1R or activation of CB2R represents promising therapeutic strategies against quetiapine-induced cardiotoxicity.

## 1. Introduction

Atypical antipsychotics, including clozapine (Clz), olanzapine (Olz) and quetiapine (Que), are common drugs for treating mental disorders such as schizophrenia, bipolar disorder, and major depressive disorder. Quetiapine, chemically similar to Clz and Olz, was approved in 1997 on the basis of clinical trials in patients with schizophrenia. According to Astra Zeneca, more than 22 million people worldwide have used Que, and it is the most-prescribed atypical antipsychotic in the United States (Traynor, 2009). Quetiapine is effective in acute and maintenance treatment of major depressive disorder and generalized anxiety

disorder, two psychotropic diseases far more common than schizophrenia or bipolar disorder. However, advisors at Food and Drug Administrator (FDA) from the United States are wary of expanding Que use due to its potential adverse events, especially metabolic problems, tardive dyskinesia and sudden cardiac death (Traynor, 2009).

To date, an increasing number of reports have shown that the clinical use of Que accompanies with side effects in the cardiovascular system, or even leads to sudden cardiac deaths (Vieweg, 2003). Compared with nonusers, the risk of sudden cardiac deaths was increased by 72% for Que (OR = 1.72, 95% CI: 1.33–2.23) (Salvo et al., 2016). This was basically similar with another population-based case-crossover

**Abbreviations:** Que, quetiapine; Clz, clozapine; Olz, olanzapine; Rimo, Rimonabant; RIP1, receptor-interacting serine/ threonine-protein kinase 1; RIP3, receptor-interacting serine/threonine-protein kinase 3; MLKL, mixed lineage kinase domain-like protein; Nec-1, necrostatin-1; CBR, cannabinoid receptor; CB1R, cannabinoid receptor 1; CB2R, cannabinoid receptor 2; AEA, anandamide; 2-AG, 2-arachidonoylglycerol

\* Corresponding authors at: Department of Forensic Medicine, School of Basic Medical Sciences, Fudan University, 138 Yixueyuan Road, Shanghai, 200032, China.

**E-mail addresses:** [lixq15@fudan.edu.cn](mailto:lixq15@fudan.edu.cn) (X. Li), [zpeng15@fudan.edu.cn](mailto:zpeng15@fudan.edu.cn) (Z. Peng), [ylzhou14@fudan.edu.cn](mailto:ylzhou14@fudan.edu.cn) (Y. Zhou), [wangj16@fudan.edu.cn](mailto:wangj16@fudan.edu.cn) (J. Wang), [linxy16@fudan.edu.cn](mailto:linxy16@fudan.edu.cn) (X. Lin), [xrdong16@fudan.edu.cn](mailto:xrdong16@fudan.edu.cn) (X. Dong), [xcliu18@fudan.edu.cn](mailto:xcliu18@fudan.edu.cn) (X. Liu), [jieqing315@fudan.edu.cn](mailto:jieqing315@fudan.edu.cn) (J. Jiang), [jiangyan@fudan.edu.cn](mailto:jiangyan@fudan.edu.cn) (Y. Jiang), [liliangli11@fudan.edu.cn](mailto:liliangli11@fudan.edu.cn) (L. Li).

<https://doi.org/10.1016/j.toxlet.2019.06.005>

Received 18 March 2019; Received in revised form 13 June 2019; Accepted 16 June 2019

Available online 18 June 2019

0378-4274/ © 2019 Elsevier B.V. All rights reserved.

study which found that use of antipsychotic drug such as Que was associated with a 1.53-fold increased risk of ventricular arrhythmia and/or sudden cardiac death. Moreover, during time windows of 7, 14, and 28 days, the above association was significantly higher among those with short-term use (Wu et al., 2015). The pathological basis underlying the clinically and forensically observed arrhythmia was in large proportion attributed to cardiac muscle disorder induced by Que (Coulter et al., 2001). According to the World Health Organization's program for international drug monitoring, Que-induced myocarditis and cardiomyopathy has been the common presentation in pathology. Myocarditis and cardiomyopathy associated with Que administration have been reported in cases and these cases might be sometimes intriguing that mimic acute ST segment-elevated myocardial infarction in practice (Roesch-Ely et al., 2002; Wassef et al., 2015). The widely reported cardiovascular side effects also raised concern from the Danish Medicine Agency or the European Medicine Agency that are consequently wary of expanding the use of Que (Jakobsen et al., 2017; Lee et al., 2013). This evidence indicates that Que-induced myocardial injury mandates further clinical and experimental investigation.

Though Que cardiotoxicity is well recognized, deep mining of this side effect with experimental evidence remains largely vacuous. Since the fundamental impact of drug-induced toxicity is to cause death of cells (Linkermann and Green, 2014), the Que-induced cardiomyocytes deaths and its regulatory mechanisms are therefore urgently needed to be uncovered.

Necroptosis is a newly defined type of programmed cell necrotic death and has been proven to be both a cause and a consequence of disease (Linkermann and Green, 2014). This form of cell death is triggered by an important mediator receptor-interacting serine/threonine-protein kinase 3 (RIP3), which is activated by receptor-interacting serine/threonine-protein kinase 1 (RIP1) upon phosphorylation and cascades to phosphorylate the downstream mixed lineage kinase domain-like protein (MLKL), leading to translocation of p-MLKL to cell membrane and consequently the plasma membrane pore-formation (Gong et al., 2017). Apart from the damage of the membrane integrity, the necrotic-like cell death is also characterized by the autophagy excess, mitochondria function loss and the reactive oxygen species generation (Xie et al., 2015). Though necroptosis and apoptosis are both forms of programmed cell deaths, they have many differences in morphological appearance and molecular pathway. Apoptosis shares morphological definition including blebbing, chromatin condensation, nuclear fragmentation, loss of adhesion and rounding (in adherent cells), and cell shrinkage. At the same time, caspase-3 mediated pathway has been activated and then leading to the activation of Bax and Bcl-2 during cell apoptosis. Unlike caspase3-mediated apoptosis, necroptosis executes cell deaths through RIP1/RIP3/MLKL signaling and the necroptotic cells show morphological features that are similar to necrosis, namely, cell swelling, organelle dysfunction and rupture of the plasma membrane (Weinlich et al., 2017). Although necroptosis may have evolved as a line of defense against intracellular infection, recent studies implicate it in a variety of disease states (Linkermann and Green, 2014). There is increasing evidence showing the significant involvements of necroptosis in drug-induced toxicity (Takahashi et al., 2012). Necroptotic cell death underlay drug-induced death of multiple cells such as primary kidney cells, neurons, retinal cells and hepatocytes (Linkermann and Green, 2014; Yuan and Kaplowitz, 2013). In particular to cardiomyocytes, the chemotherapeutic drug dasatinib-induced cardiotoxicity acted via leading cardiomyocytes to HMGB1-mediated necroptosis (Xu et al., 2018). Necroptosis mediators RIP1/RIP3 were found to be highly expressed in cardiomyocytes in the acute viral insult and that pharmacologic blockade of the necroptosis pathway using its specific blocker Necrostatin-1 (Nec-1) dramatically reduced the myocardial damage (Zhou et al., 2018).

We have previously reported that Que, as well as other antipsychotics Clz, Olz and chlorpromazine, associated with inflammation-featured diseases (*i.e.* pneumonia or myocarditis) with these drugs

administration (Li et al., 2018). Clozapine-induced cardiotoxicity caused opposing effects on cannabinoid receptors (CB1R and CB2R) expression (Li et al., 2019). The present study sought to investigate the cardiac side effects after Que use with a first-hand experimental murine model. Quetiapine-induced cell deaths were systemically assessed and based on this assessment; we further evaluated the potential of cannabinoid receptor antagonists/agonists in rescuing Que-induced cardiomyocyte death. Our data represented the first one, to the best knowledge of us, to report experimental evidence linking Que cardiotoxicity with induced necroptotic cell death, and we proposed that selective CB1R antagonists or CB2R agonists opened beneficial clues towards Que cardiac toxic effects by inhibiting necroptosis.

## 2. Materials and methods

### 2.1. Animal experiments

All animal experiments were conducted according to the Care and Use of Laboratory Animals of the NIH Guide (NIH Publication No. 85-23, revised 1996). Protocols for the animal experiments were approved by the Institutional Animal Care and Use Committee at the School of Basic Medical Sciences, Fudan University (No.: 20170223-004). All efforts were made to minimize animal suffering. Male Balb/C mice at the age of ~ 4-week old were purchased from SLAC Inc. (Shanghai, China) and habituated for 1 week. All mice were housed in a sterile laboratory animal breeding condition and were maintained under suitable temperature with an alternant 12h light-dark cycle. Food and water are available to them. At 15:00 of each day, mice were intraperitoneally injected with 100  $\mu$ L of vehicle (PBS) (Control group, Ctrl) or Que (60 mg/kg). For the experimental design, some groups of mice were co-treated with inhibitors which were pretreated approximately 1 h before the injection of Que or PBS (see the flowchart in Fig. 1A). Mice weights were recorded on a daily basis before injection unless otherwise stated. The number of mice was 5–6 per group as stated in each figure legend. Treatments lasted for consecutive 21-days. On the 21th day, all mice had blood collected *via* orbital vein to prepare serum samples, while at the same time; the tibia length (TL) and heart weight (HW) were measured. Hearts were transversely dissected and part of the heart tissues was subject to formalin fixation and paraffin embedding for heart slicing. The remaining heart tissues were stored at -80°C until use.

### 2.2. Histological examination

Heart slices were stained with Hematoxylin and Eosin (HE) staining and PicroSirius Red (PSR) staining for histological observation of inflammation infiltration and fibrotic lesions, respectively. For the purpose of this study, myocarditis was defined as  $\geq 1$  collection of inflammatory cells with each collection a minimum of 10 cells. The inflammatory infiltrates were classified in terms of the degree of cellular infiltration and graded on a 5-point scale ranging from 0 to 4+ (inflammation infiltration index) as we have previously described (Li et al., 2019): 0, no or questionable; 1+, 1–2 foci; 2 to 3+, intermediate severity with multifocal lesions; 4+, coalescent and extensive lesions over the entire examined heart tissue. Sparse infiltration of inflammatory cells was also scored as 4+. After PSR staining, for quantifying the extent of fibrosis, a random of 5 fields from each group of mice hearts were selected and photographed. The fibrosis area was then automatically analyzed in proportion to the slice area using Image J software (National Institute of Health, Bethesda, MD, USA). Multiplexed immunohistochemistry (IHC) analysis was performed using the Opal™ multicolor IHC kit (PerkinElmer Inc., Boston, MA, USA) according to previous description (Stack et al., 2014). Briefly, the RIP3 primary antibody (Catalog No.: 17563-1-AP) and monoclonal MLKL antibody (Catalog No.: 66675-1-Ig) were purchased from Proteintech (Rosemont, IL, USA) and incubated with the heart slices. The RIP3 and MLKL were

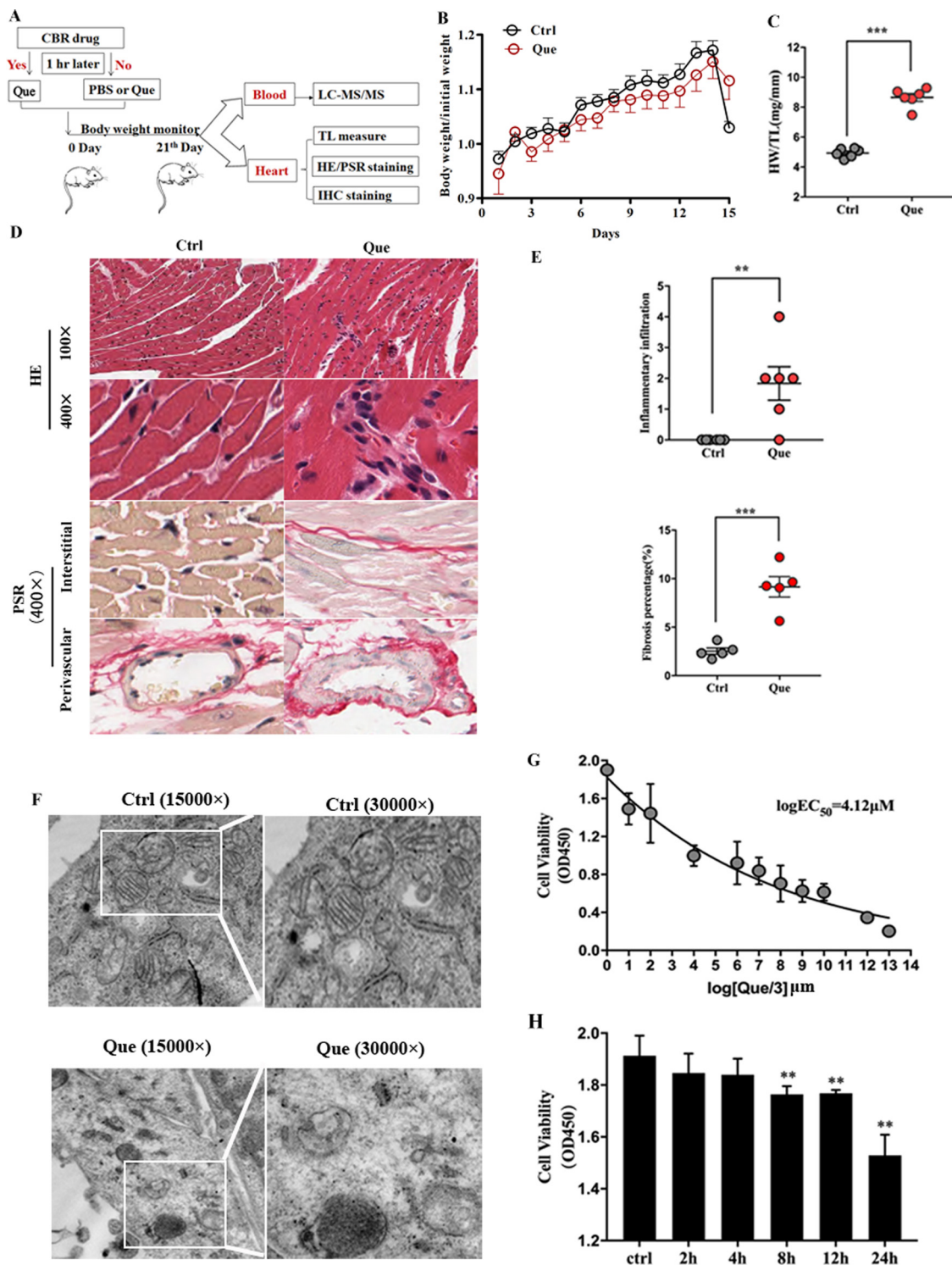


**Fig. 1.** Quetiapine (Que) induced myocardial injury *in vivo* and *in vitro*. (A) Flowchart of experimental design. (B) Body weights were monitored in Ctrl or Que-treated mice on a daily basis. (C) The HW/TL ratio was calculated after 21-day continuous treatments (n = 6/group). (D) Quetiapine treated hearts showed remarkable inflammatory infiltration (HE staining) and fibrosis in both perivascular and interstitial areas (PSR staining). (E) Quetiapine treatments significantly increased the inflammatory infiltration index (n = 6/group) and the fibrosis percentage (%) (n = 5/group). (F) Transmission electron microscope (TEM) showed that control cardiomyocytes presented normal subcellular structures, while Que-exposed cells presented with disintegrity of cell membrane and mitochondria swelling. (G) Serial doses of Que were added to myocardial HL-1 cells, and cell viability was monitored using CCK-8 kit after 24 h incubation. The F value was 1.353 and the p value was 0.2488 for Brown-Forsythe test of variance homogeneity. The EC<sub>50</sub> equals to 104.12 μM. (H) Quetiapine (2 μM) was incubated with HL-1 cells for serial hours (0 h, 2 h, 4 h, 8 h, 12 h, and 24 h). Cell viability was assessed using CCK-8 kit. The F value was 0.3818 and p value was 0.8502 for Brown-Forsythe test of variance homogeneity. Ctrl, Control. Que, quetiapine. HW/TL, heart weight/tibia length. HE, hematoxylin and eosin. PSR, PicroSirius Red. \*p < 0.05, \*\*p < 0.01, \*\*\*p < 0.001 vs. Ctrl.

visualized by pink and brown signals, respectively.

### 2.3. Antibodies

Primary rabbit monoclonal antibodies against CB1R (Catalog No.: 93815) and RIP1 (Catalog No.: 3493) were purchased from Cell Signaling Technology (Boston, MA, USA). Anti-Bax (Anti-Bax into 2772) primary rabbit antibody was as well purchased from Cell Signaling Technology. Primary rabbit polyclonal anti-CB2R antibody was purchased from Gene Tex Inc. (Catalog No.: GTX23561, Irvine, CA, USA). Primary rabbit monoclonal antibody against LC-3B (Catalog No.: 192890) and phosphorylated MLKL (S345) (Catalog No.: 196436) were purchased from Abcam Cambridge, United Kingdom. Primary antibodies against Caspase 3 (Catalog No.: 19677-1-AP), Bcl-2 (Catalog No.: 12789-1-AP), RIP3 (Catalog No.: 17563-1-AP), MLKL (Catalog No.: 66675-1-Ig and 21066-1-AP), Beclin 1 (Catalog No.: 11306-1-AP), were purchased from Proteintech Inc. (Rosemont, IL, USA). A mouse monoclonal antibody against  $\beta$ -action was purchased from Santa Cruz Biotechnology (Catalog No.: sc-47778, Santa Cruz, CA, USA). HRP-linked secondary antibodies were purchased from Jackson laboratories Inc. (West Grove, PA, USA). Goat anti-rabbit secondary antibody Alexa Fluor 555 (Catalog No.: A-21428) and Alexa Fluor 488 (Catalog No.: A-11008) were purchased from Invitrogen Inc. (Carlsbad, CA, USA). The application of all primary antibodies into the present assays was validated by manufactures.

### 2.4. Chemicals and solutions

Antipsychotic Clz was purchased from Sigma-Aldrich (St. Louis, MO, USA). Clozapine was dissolved in 0.1 M HCl and pH balanced in phosphate buffered saline (PBS) to make a stock solution of Clz (80 mM). The stock solution was then diluted based on use dosage. A selective CB1 antagonist Rimonabant (Rimo) and selective CB2 antagonist AM 630 were commercially obtained from Sigma-Aldrich. A selective CB1 antagonist AM 281 (Catalog No.: B6603) and selective agonist ACEA (Catalog No.: 1319) were purchased from APEXBio Technology (Boston, MA, USA) and Tocris Bioscience (Abingdon, OX, UK), respectively. Another CB2 agonist JWH-133 was purchased from MedChemExpress (Catalog No.: 259869-55-1, Monmouth Junction, NJ, USA). ACEA, Rimo and AM 630 were prepared as 1 mg/mL, 0.6 mg/mL and 1 mg/mL working solutions, respectively in solvents composing of DMSO, Tween-20 and PBS. A selective CB2 agonist AM 1241 was purchased from Selleck Chemicals (Houston, TX, USA) and prepared as 10 mg/mL working solution in solvents composing of DMSO and PBS. The highest final concentration of DMSO in external solution was  $\leq 1\%$ , a concentration that had no effect on mice survival. Quetiapine fumarate and Olz (Catalog No.: S2493) were purchased from Selleck Chemicals and dissolved in saline added with 1% acetic acid to make stock solutions (12 mg/mL, 0.5 mg/mL, respectively). Necrostatin-1 (Nec-1) was purchased from Santa Cruz Biotechnology (Catalog No.: 4311-88-0) and was dissolved to 1 mg/mL for working concentration. Final doses for *in vivo* experiments were Rimo (3 mg/kg), AM 281 (2.5 mg/kg), ACEA (5 mg/kg), AM 1241 (5 mg/kg), JWH-133 (5 mg/kg), and AM 630 (5 mg/kg), respectively.

### 2.5. Cell culture

Myocardial HL-1 cells were maintained in our laboratory and were cultured in dulbecco's modified eagle medium (DMEM) supplemented with 10% fetal bovine serum (FBS). For the *in vitro* model of Que toxicity, HL-1 cells were treated with different doses of Que from low-dose (LD, 1  $\mu$ M), medium-dose (MD, 2  $\mu$ M) to high-dose (HD, 4  $\mu$ M) under an incubator at 37°C for 24 h. Cells were also treated with a fixed dose (2  $\mu$ M) but with Que exposure lasting from 0, 2, 4, 8, 12, 24 to 36 h, respectively. To assess the effects of Nec-1 (60  $\mu$ M) or CBRs agents on Que toxicity, HL-1 cells were pretreated with Nec-1 or indicated CBR

modulators. The final doses of Nec-1 (60  $\mu$ M), Rimo (2  $\mu$ M), AM 281 (2  $\mu$ M), AM 1241 (5  $\mu$ M), JWH-133 (1  $\mu$ M) were applied to the medium 30 min prior to application of Que.

### 2.6. Western blot assay

Cardiomyocyte cultures were lysed with RIPA buffer (Beyotime, Nantong, China) mixed with protease/phosphatase inhibitor cocktail (Cell Signal Technology). The total protein was quantified using a BCA kit (Thermo Scientific, CA, USA) according to the manufacturer's protocol. An equal amount of protein was then loaded to each lane on a 10% SDS-PAGE gel and transferred to polyvinylidene fluoride (PVDF) membrane. Then the bolts were blocked in 5% skim milk dissolving in tris-buffered saline with 0.1% Tween-20 (TBST) for 1 h at room temperature, probed with the primary antibody including overnight at 4°C. Blots were then washed in TBST for twice, and incubated with the secondary antibody (1:50,000, Jackson Laboratories) diluted in 5% milk for 1 h.  $\beta$ -actin was synchronously detected for loading control. The intensity was quantified using the Image J software and normalized to  $\beta$ -actin or ATP1 $\alpha$ 1 as indicated.

### 2.7. Extraction of membrane, nuclear and cytoplasmic protein

For analysis of subcellular components, membrane, nuclear and cytoplasmic proteins were extracted using a commercial kit from the Sangon Biotech (Catalog No.: C510002, Shanghai, China) according to the manufacturer's instructions. Briefly, through a cell pulp protein extraction reagent, cells were fully inflated and the cell membrane was destroyed so that the cytoplasmic protein was released. Then the nuclear proteins were collected from the supernatant after centrifugation at 4°C, 12,000 rpm for 10 min. The precipitates were then cracked using ultra sonication and the membrane protein was obtained after centrifugation at 4°C, 12,000 rpm for 10 min.

### 2.8. Immunofluorescence assay

Mouse myocardial HL-1 cells were cultured in 24-well plates and received Que treatment (final concentration = 2  $\mu$ M) alone or in combination with indicated agent co-incubation. After 24 h incubation, cells were fixed with pure acetone for 10 min and washed with iced PBS for three times. After blocking with goat serum for 1 h, cells were co-incubated with primary antibody against MLKL at 4°C overnight. Alexa Fluor goat anti-mouse IgG was included as the secondary antibody. DAPI was counterstained at a dilution of 1:1000 for 10 min at room temperature.

### 2.9. Transmission electron microscope

Myocardial HL-1 cells were incubated with Que (2  $\mu$ M) or PBS for 24 h in a 6-cm dish. Culture medium was then discarded and cells were trypsinized and precipitated by centrifuge at 1000 rpm for 5 min. Cell precipitates were then immersed in 2% glutaraldehyde. The images were taken by transmission electron microscope (TEM) (FEI/PHILIPS CM120 TEM, Philips Electron Optics B.V.).

### 2.10. Cell viability assay

To assess the effects of Que on myocardial cell viability, cells were seeded into 96-well plates and treated as indicated. Cell number was monitored by detecting the absorbance of each well. On each monitored time points, an aliquot of 10  $\mu$ L CCK-8 solution (Beyotime, Nantong, China) was added into the culture medium. Cells were then re-incubated at 37°C for additional 2 h. The absorbance at a wavelength of 450 nm (OD450) was detected on a microplate reader (BioTek, Winooski, VT, USA).

### 2.11. Detection of major endocannabinoid levels by LC–MS/MS

Myocardial HL-1 cells were cultured in 6-well plates and treated with Que (2  $\mu$ M) for 24 h when cells reached ~80% confluence. Following lipid extraction of cultured cells or serum samples, the levels of anandamide (AEA) and 2-arachidonoyl glycerol (2-AG) were quantified by LC–MS/MS as we described previously (Dong et al., 2018).

### 2.12. Statistical analysis

Data were displayed as mean  $\pm$  standard error of means (SEM). The Students' *t*-test was used for comparison of means between groups, while one-way analysis of variance (ANOVA) was used for comparisons of  $\geq 3$  groups, followed by a least significant difference (LSD) post-hoc test. In the ANOVA analysis, normal distribution was initially analyzed and then Brown-Forsythe test was used for analysis of homogeneity of variance when necessary. A *p* value of less than 0.05 was considered to be statistically significant.

## 3. Results

### 3.1. Chronic exposure of Que induced cardiotoxicity in vivo and in vitro

Antipsychotics have been widely documented to prolong the corrected QT interval in clinic or even lead to sudden cardiac death (Wu et al., 2015). The histopathology of Que cardiotoxicity remains rarely reported. In this experimental study, we used 60 mg/kg of Que, a dose comparable to clinical maintenance use, to intraperitoneally inject mice. During the continuous treatment, Que-treated mice did not show significant body weight changes with PBS-treated counterparts (Fig. 1B). The ratio of heart weight to tibia length (HW/TL) is an index reflecting interstitial edema and cardiac pathology. Calculation of HW/TL showed that it was significantly increased to approximate 2-fold after chronic Que treatment (Fig. 1C). Mice hearts were harvested for histological analysis. By contrast to PBS-treated control hearts, HE staining showed that Que-insulted heart showed focal to multifocal inflammatory cells accumulation (Fig. 1D, HE staining). PSR staining (400 $\times$ ) further showed that fibrotic tissues remarkably accumulated in both perivascular and interstitial areas of Que-treated hearts (Fig. 1D, PSR staining). The inflammatory infiltration index significantly increased as compared with control mice (Fig. 1E, upper panel, *p* < 0.01). Quantification of fibrosis showed that the area of fibrotic tissues in Que-exposed hearts was approximately 3-fold of that in Que-free control hearts (Fig. 1E, lower panel, *p* < 0.001). In the cultured cardiomyocytes, transmission electron microscope revealed that control cells showed normal subcellular structures, whereas Que-treated cells showed disintegrity of cell membrane, mitochondrial swelling and reticulum expansion (Fig. 1F). In addition, Que-induced cell deaths were dose-dependent (Fig. 1G) and time-dependent (Fig. 1H), conforming to the clinical observation that long-term or higher dose of Que predispose to cardiotoxicity (Adameova et al., 2017). All these results suggested that Que indeed induced cardiotoxicity.

### 3.2. Quetiapine induced cardiomyocyte cell necroptosis

In view that Que induced mitochondrial swelling, disintegrity of cell membrane, and reticulum expansion, it was hypothesized that Que predisposed cells to necrotic-like deaths. Necroptosis is characterized by the cascade activation of RIPs and the phosphorylation of MLKL which eventually translocates to cell membrane and lead to pore formation (Cai et al., 2014). Initially, we treated cardiomyocytes with three common atypical antipsychotics (Clz, Olz and Que) and detected the activation of necroptosis. The result showed that Que exerted consistent promotion effects on the necroptosis signaling proteins as well as the phosphorylation of MLKL (Fig. 2A), indicating that Que could induce cell necroptosis. Then we incubated myocardial HL-1 cells

with Que for different doses (Fig. 2B) or different hours (Fig. 2C). The Que-induced activation of necroptosis was dose and time-dependent. To investigate the activation of necroptosis in mice hearts, the multiplexed IHC analysis was conducted to co-stain RIP3 and MLKL (Fig. 2D). It was visible that RIP3 (pink) and MLKL (brown) were dramatically increased within myocardium and importantly, MLKL was observed to translocate from cytoplasm in intact heart to cell membrane in Que-insulted heart (Fig. 2D). Quetiapine-induced translocation of MLKL was further confirmed by immunofluorescence staining of cells (Fig. 2E). Counting of cells with MLKL-gathering cytomembrane revealed that after 24 h exposure, Que increased the percentage of cells with membrane MLKL-positive location by approximate 5-folds (Fig. 2F). These observations suggested that Que induced necroptotic cell deaths when causing side cardiac effects.

### 3.3. Quetiapine had minimal effects on cell apoptosis or autophagy

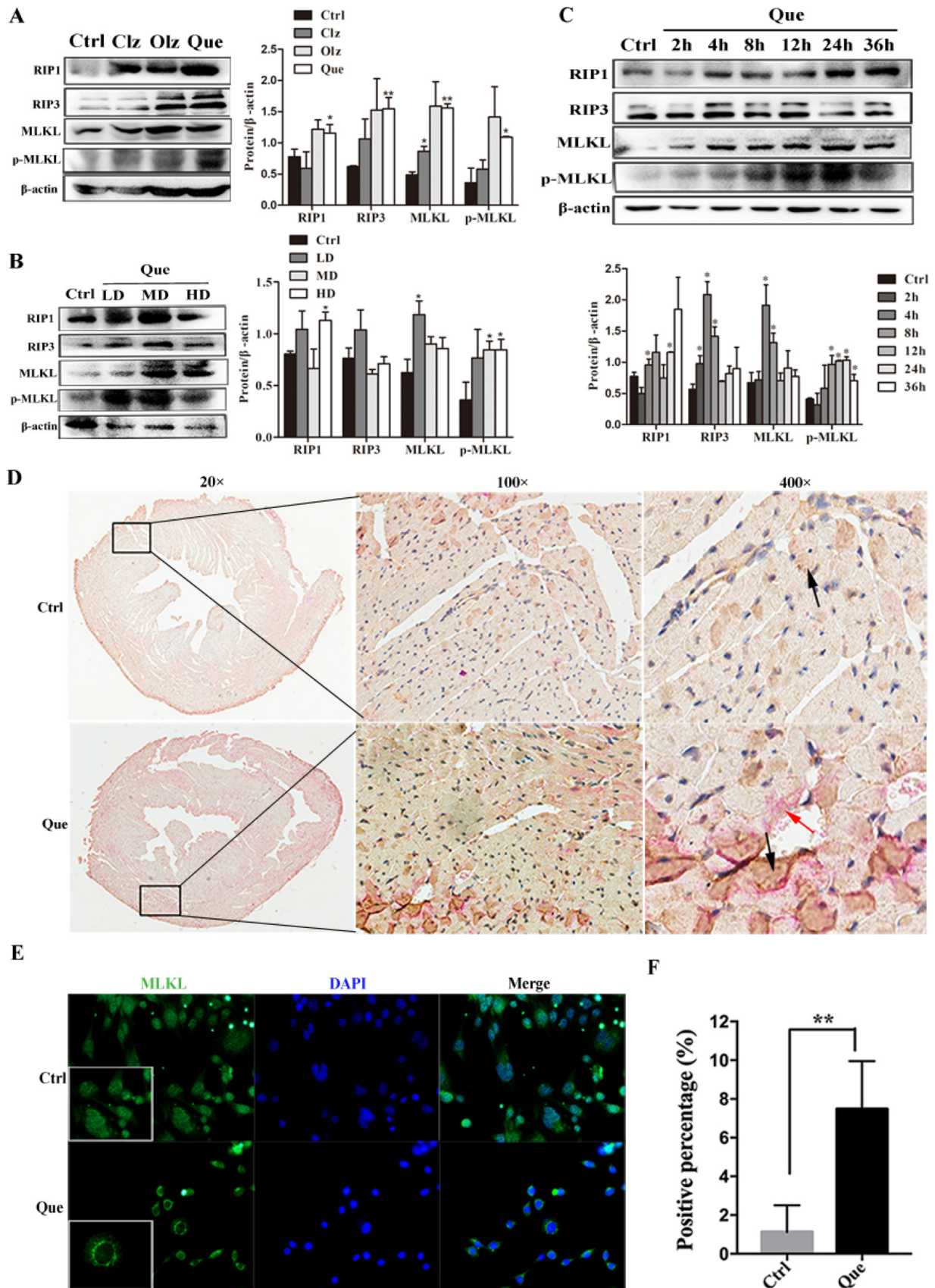
Next, the effects of Que on other types of cell deaths were investigated. Cells were incubated under the same condition as above. Cell apoptosis markers such as caspase 3 and Bcl-2 remained stable across Que treatments. Pro-apoptotic Bax tended to remain unchanged across Que doses or treatment hours (Fig. 3A and B). The conversion of LC3B-I to LC3B-II is a marker of autophagy activation (Huang and Liu, 2015; Romao and Munz, 2014). It was observed that the LC3B-II levels did not increase by Que treatments. Instead, it tended to decrease upon increasing Que doses or extending insult hours (Fig. 3C–D). Beclin 1 also remained unremarkably changed throughout all groups (Fig. 3C and D). Together with the above data, it could be concluded that Que stably induced cell necroptosis.

### 3.4. Pharmacologic inhibition of necroptosis protected against Que cardiotoxicity

Necrostatin-1 (Nec-1) is a well-recognized inhibitor of necroptosis which specifically inhibited the activation of RIP1 (Szobi et al., 2016). The efficiency of Nec-1 to block necroptosis was also verified in our cultured cardiomyocytes (Fig. 4A). Then Nec-1 was pretreated to mice each time before the start of Que injection. At the end of treatments, heart sections were subject to histological examination and it was shown that Nec-1 visibly rescued Que-induced myocardial injury (Fig. 4B). As a reflection of heart pathology attenuation, the HW/TL was significantly decreased in response to Nec-1 pretreatments (Fig. 4C, *p* < 0.01). Inflammation index tended to be milder (Fig. 4D) and the fibrosis accumulation was evidently relieved by Nec-1 pretreatments (Fig. 4E). These data implicated that inhibition of necroptosis attenuated Que cardiotoxicity.

### 3.5. Quetiapine treatments imbalanced the endocannabinoid system

The endocannabinoid system has been widely reported to involve in drug toxicity (du Plessis et al., 2015; Fernandez-Ruiz et al., 2015; Gerra et al., 2010). To further probe whether cannabinoid receptors (CBRs) transduce extracellular Que toxicity to intracellular responses, we collected the serum samples from control and Que-treated mice, and detected the levels of anandamide (AEA) and 2-arachidonoylglycerol (2-AG) with our developed LC–MS/MS method (Dong et al., 2018). The content of AEA appeared to be decreased after Que exposure (Fig. 5A). 2-AG, the most enriched endocannabinoid, was significantly decreased in Que-treated mice as compared to their counterparts (Fig. 5B). Likewise, in the cultured cardiomyocytes, the level of 2-AG decreased by almost 50% after 24 h treatment of Que (Fig. 5C). Moreover, the effects of Que on two subtypes of CBRs (CB1R and CB2R) were evaluated. The results showed that the total protein levels of CB1R downregulated, while that of CB2R upregulated with the doses increased or treatment hours extended (Fig. 5D). CBRs function mainly through shuttling between membrane and cytoplasm (Pertwee, 2015). The membrane and



(caption on next page)

**Fig. 2.** Quetiapine (Que) induced necroptotic cell death in hearts. (A) Western blot analysis detected necroptosis related mediators in Ctrl, Clz (40μM), Olz (1μM), and Que (2μM)-treated HL-1 cells. The intensity of blots was quantified at right panel. Quetiapine induced consistent promotion of RIP1, RIP3, MLKL and p-MLKL levels among all drugs. (B) Quetiapine in the dose range of 1 μM (Low dose, LD) to 4 μM (High dose, HD) gradually elevated the levels of RIP1, RIP3, MLKL and p-MLKL after 24 h treatment. The medium-dose (MD) of Que (2 μM) gave rise to the most activation of necroptosis. Right panel showed the quantified data after ImageJ analysis of intensity. (C) Quetiapine (2 μM) increasingly promoted the RIP1, RIP3, MLKL, and p-MLKL levels in HL-1 cells with extended treatment durations (2, 4, 8, 12, 24 and 36 h). Each blot was quantified using ImageJ software. (D) Multiplexed IHC analysis of RIP3 (pink) and MLKL (brown) in Ctrl or Que (60 mg/kg)-treated mice heart slices. MLKL translocated from cytoplasm in Ctrl heart to cell membrane in Que-treated heart (black arrow), while RIP3 presented with high expression exclusively in Que-treated hearts. (E) Immunofluorescence assay detected the localization of MLKL in Ctrl or Que (2μM)-treated myocardial HL-1 cells. DAPI was co-stained to reveal cellular nucleus. Magnification: 400 × . (F) Necroptotic cells were denoted as those with MLKL-gathering membrane. Percentage of cell necroptosis was calculated as the rate of necroptotic cells in all cell numbers (DAPI-positive cells). Ctrl, control. Clz, clozapine. Olz, olanzapine. Que, quetiapine. \*,  $p < 0.05$ ; \*\*,  $p < 0.01$  vs. Ctrl.

cytoplasmic proteins were then extracted respectively and subject to western blot analysis. Interestingly, our results showed that the protein level of CB1R gradually decreased on cell membrane but shuttled to cytoplasm (Fig. 5E). On the contrast, the CB2R enriched on cell membrane and significantly decreased in cytoplasm (Fig. 5E). All these results suggested that Que regulated two subtypes of CBRs in bidirectional ways in myocardium.

**3.6. CB1R antagonists, but not its agonist alleviated Que-induced toxic effects**

Next, selective CB1R antagonists AM 281 and Rimo and its agonist ACEA were used. In the CB1R antagonists' pretreatments, either Rimo or AM 281 attenuated Que-induced histopathology (Fig. 6A). The HW/TL was significantly decreased after either CB1R antagonist

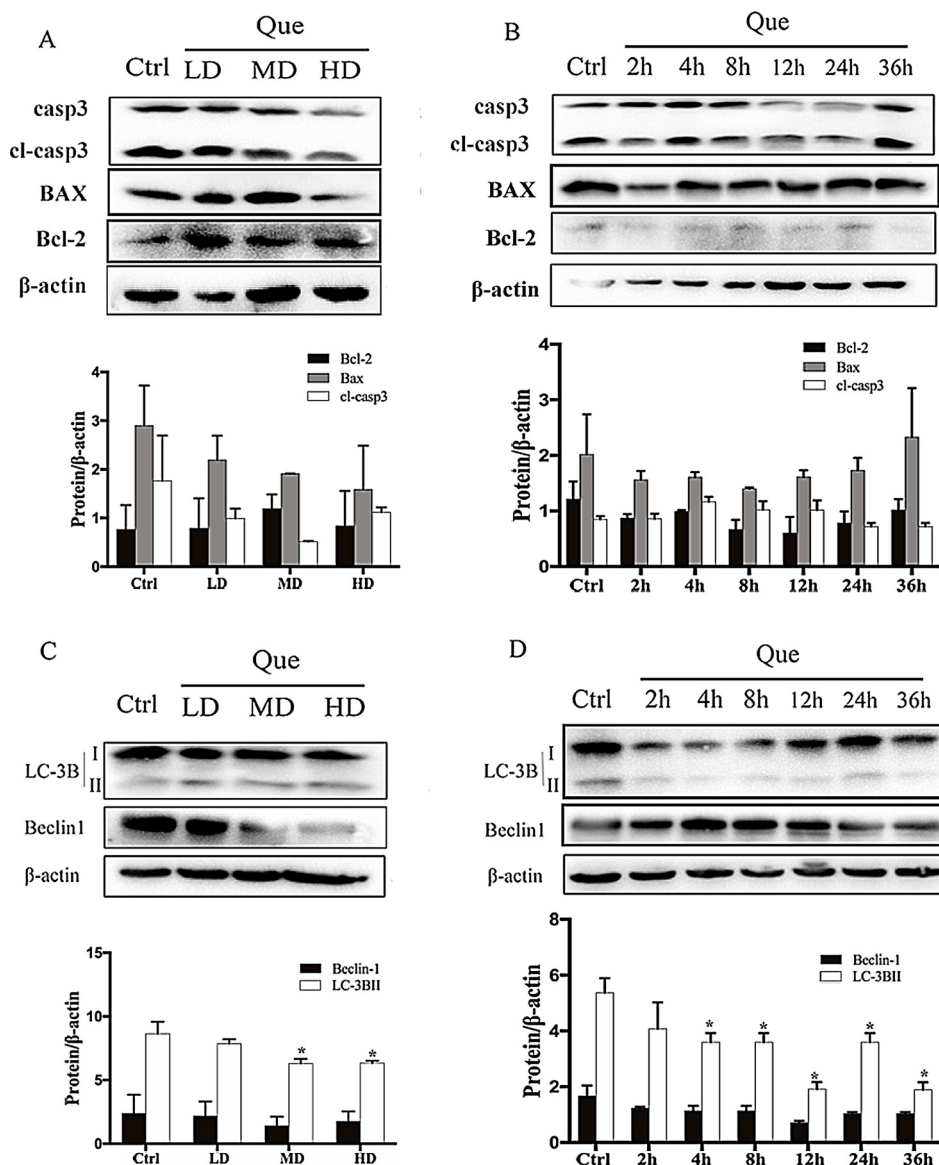


**Fig. 3.** Quetiapine (Que) exerted minimal effects on cardiomyocyte apoptosis and autophagy. (A, B) Cardiomyocytes were exposed with low dose (LD, 1 μM), medium dose (MD, 2 μM) and high dose (HD, 4 μM) of Que, respectively, or were treated with a constant Que dose (2 μM) for different hours. Cell apoptosis markers including caspase 3 (both cleaved form and its total level), Bax and Bcl-2 were detected. (C, D) Cardiomyocytes were treated as above stated. Autophagy markers including LC3B and Beclin 1 were detected. Each blot of the panels was quantified using ImageJ software and shown at the lower panels. \*,  $p < 0.05$  vs. Ctrl.

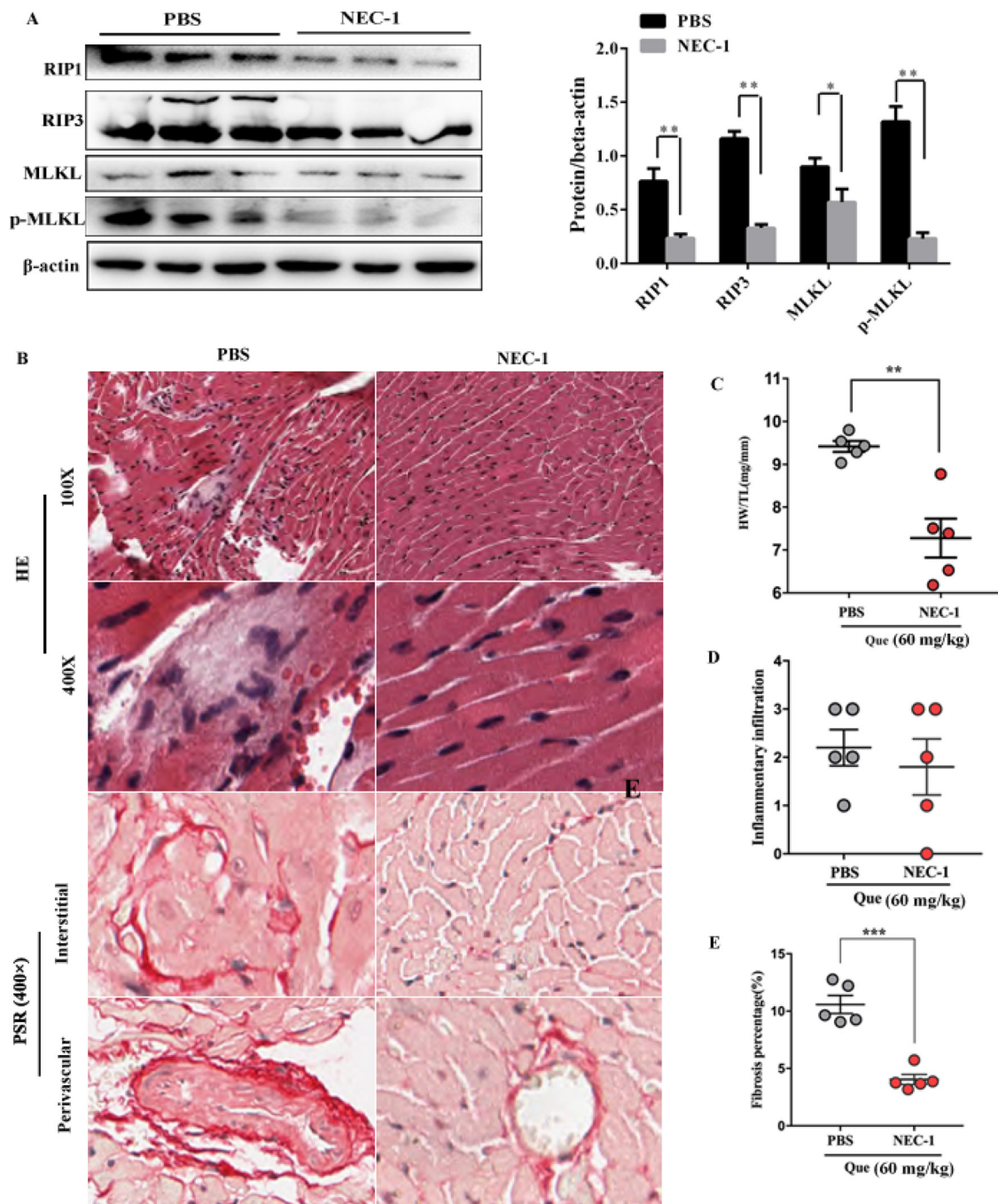


**Fig. 4.** Inhibition of necroptosis alleviated Quetiapine (Que)-induced cardiotoxicity. (A) Western blot assay confirmed that Nec-1 was valid to inhibit the process of necroptosis via blocking the RIP1 activation. The intensity of each blot was quantified using ImageJ as shown in the right panel. (B) The Que-treated mice were preinjected with vehicle (Veh, PBS) or Nec-1 (Nec-1 group) 1 h before Que treatment. At the end of experiments, mice hearts were cut into slices for histological analysis including HE staining and PSR staining. Quetiapine-induced cardiopathy including inflammatory infiltration (HE staining) and fibronectin accumulation (PSR staining) were histologically alleviated by Nec-1 pretreatments. (C–E) Effects of Nec-1 pretreatments on the HW/TL ratio, the inflammatory infiltration index and the fibrotic area percentage (%) in Que-exposed hearts (n = 5/group). Nec-1, necrostatin-1. HE staining, hematoxylin and eosin staining. PSR, PicroSirius Red. HW/TL, heart weight to tibia length. \**p* < 0.05, \*\**p* < 0.01, \*\*\**p* < 0.0001 as indicated.

pretreatment (Fig. 6B). Inflammation and fibrosis were also rescued by the CB1R antagonists (Fig. 6C and 6D). On the contrary, the pretreatment of ACEA remarkably worsened the Que-induced myocardial injury (Fig. 6E). The HW/TL was significantly increased (Fig. 6F) and inflammation infiltration was evidently promoted by ACEA treatments (Fig. 6G). Fibrotic tissues also appeared to extend by area in ACEA-pretreated hearts (Fig. 6H). The results demonstrated that inhibition of CB1R could be therapeutic against Que cardiotoxicity.

### 3.7. CB2R agonists, but not its antagonist blunted Que-induced toxic effects

In addition, selective CB2R agonists JWH-133 and AM 1241 and its antagonist AM 630 were tested. In the CB2R agonists' pretreatments, either JWH-133 or AM 1241 attenuated the histopathology induced by Que as evidenced by HE staining and PSR staining (Fig. 7A). The HW/TL was significantly decreased by either CB2R agonist pretreatment (Fig. 7B). Inflammation infiltration and fibrotic accumulation were also suppressed by the CB2R agonists (Fig. 7C and D). Reversely,

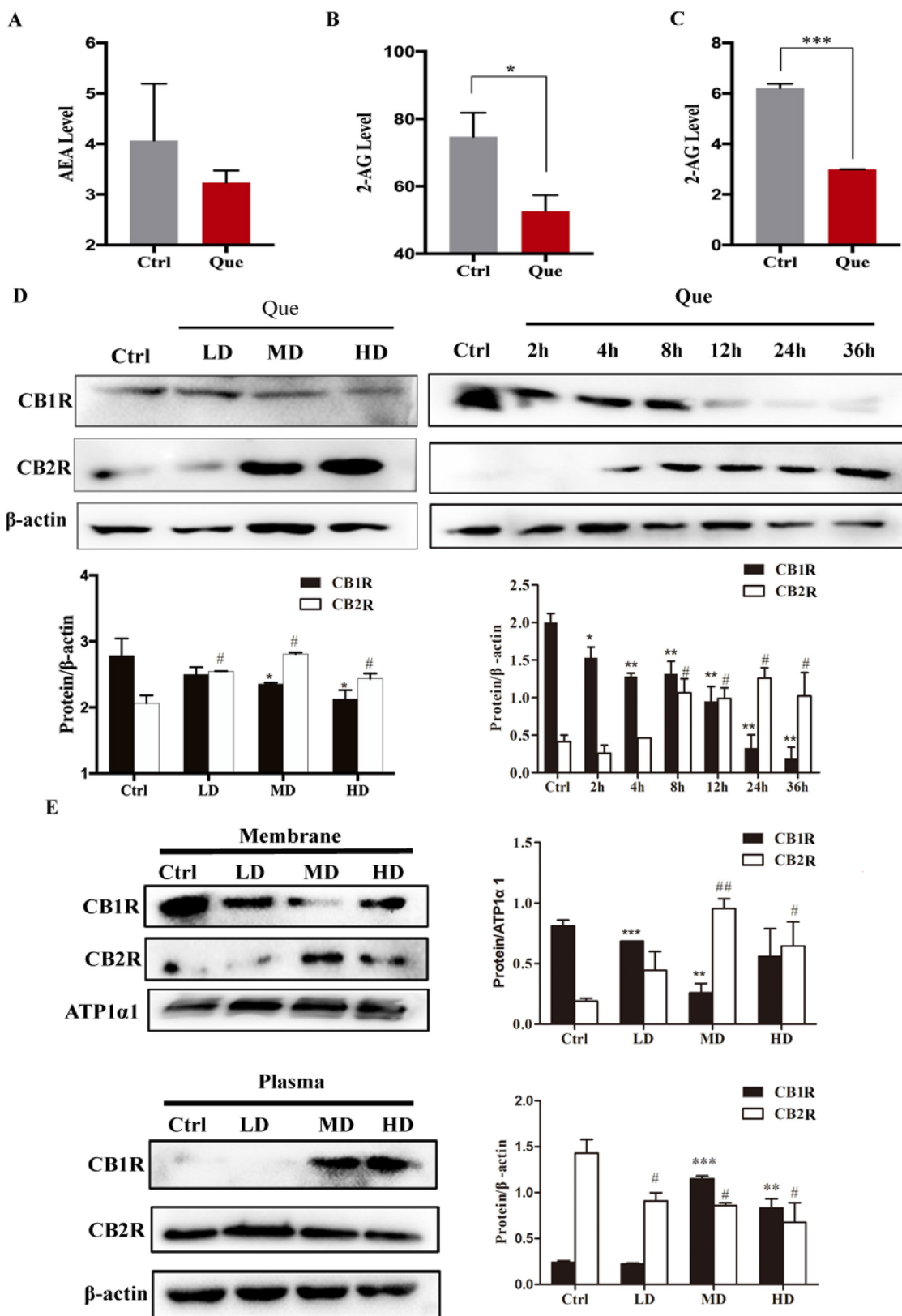


**Fig. 5.** Chronic treatment of Que imbalanced the endocannabinoid system. (A, B) Serum levels of AEA and 2-AG in control or Que (60 mg/kg)-treated mice using LC-MS/MS (n = 5 mice/group). (C) The levels of 2-AG were detected in control and Que (2 μM)-treated HL-1 cardiomyocytes by LC-MS/MS. (D) Western blot analysis of the total protein levels of CB1R and CB2R in cultured HL-1 cells. Each blot of the panels was quantified using ImageJ software and shown at lower panels. Changes of Que doses (from 1 μM to 4 μM) or its exposure time (0, 2, 4, 8, 12, 24 and 36 h) caused the opposing effects on CB1R and CB2R protein levels. (E) Subcellular components of HL-1 cells were separated and collected. CB1R and CB2R located at cytomembrane and cytoplasm were then blotted. ATP1α1 and β-actin were synchronously detected as the inner control for membrane and plasma, respectively. The intensity of blots was quantified and shown at right panels. \*, p < 0.05; \*, p < 0.01; \*\*\*, p < 0.001 vs. Ctrl in CB1R groups and #, p < 0.05; ##, p < 0.01 vs. Ctrl in CB2R groups.

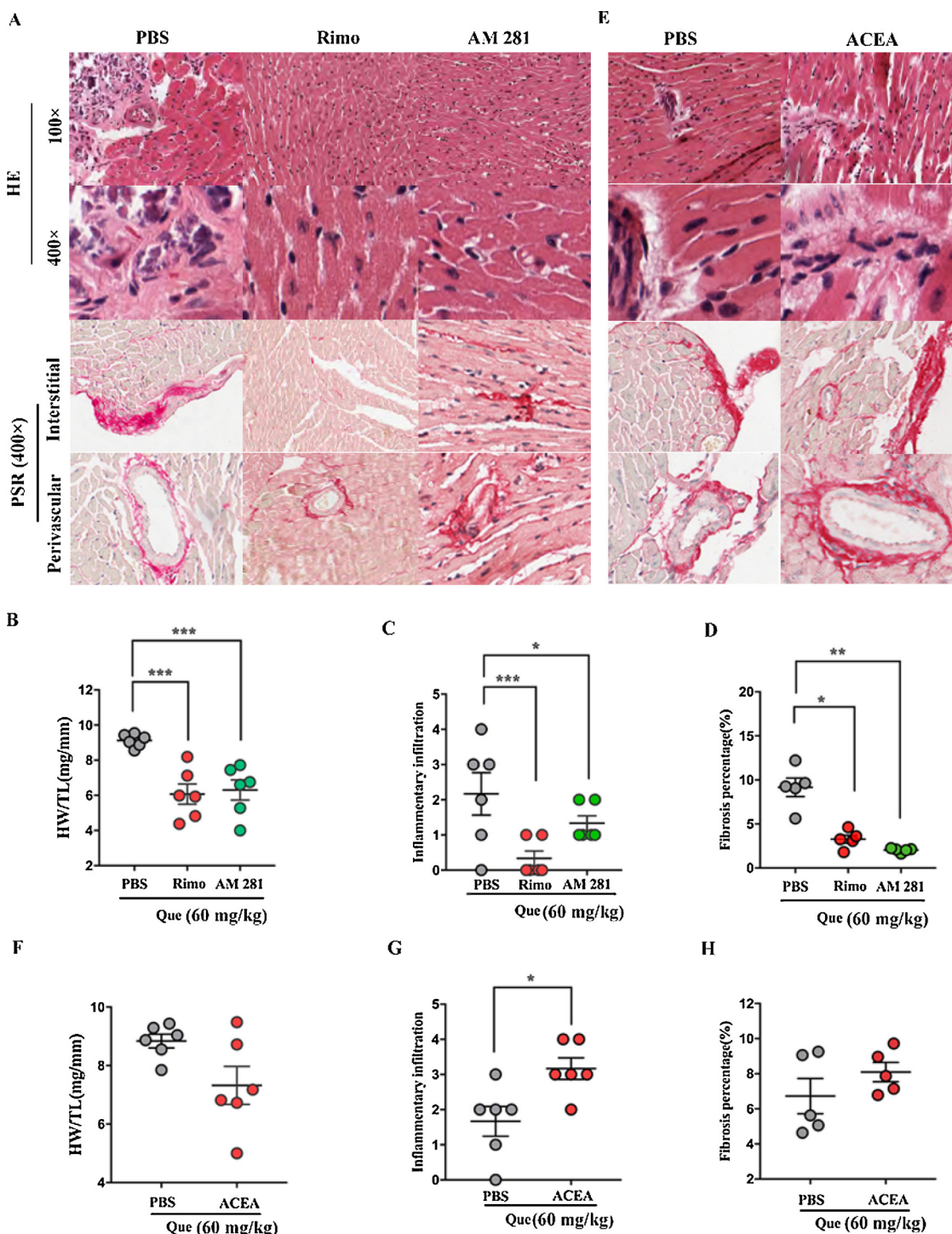


**Fig. 6.** Pharmacologic inhibition of CB1R protected against Que cardiotoxicity. (A) In a first experimental set, mice were pretreated with PBS, CB1R antagonists Rimo or AM 281 (n = 6 mice/group) before the start of Que insult. Twenty-one days after treatments, mice were sacrificed. Heart sections were stained with HE and PSR reagents for histological examination. Blockade of CB1R remarkably relieved the heart inflammation infiltration and fibrosis. (B) Mouse HW/TL was calculated for PBS, Rimo, or AM 281-pretreated group. (C, D) Inflammation index and percentage of fibrosis were calculated for each group of mice. (E) In a second experiment, mice were pretreated with PBS or the specific CB1R agonist ACEA (n = 6 mice/group) 1 h before the start of Que insult. Heart sections were stained with HE or PSR reagents for histological examination. (F) The HW/TL was calculated for each group of mice after sacrifice. (G, H) Inflammation index and the extent of fibrosis were calculated for PBS or ACEA-pretreated mice. Rimo, Rimonabant. HE staining, hematoxylin and eosin staining. PSR, PicroSirius Red. HW/TL, heart weight/tibia length. \**p* < 0.05, \*\**p* < 0.01, \*\*\**p* < 0.001 as indicated.

pretreatment of AM 630 seemed not to relieve the inflammation but worsened the Que-induced fibrosis in the perivascular areas (Fig. 7E). Though the HW/TL ratio (Fig. 7F) and inflammation infiltration index (Fig. 7G) were not significantly different between hearts with and without AM 630 treatments, the extent of fibrosis significantly

worsened in ACEA-pretreated hearts (Fig. 7H). The results demonstrated that CB2R agonists had beneficial effects against Que cardiotoxicity.

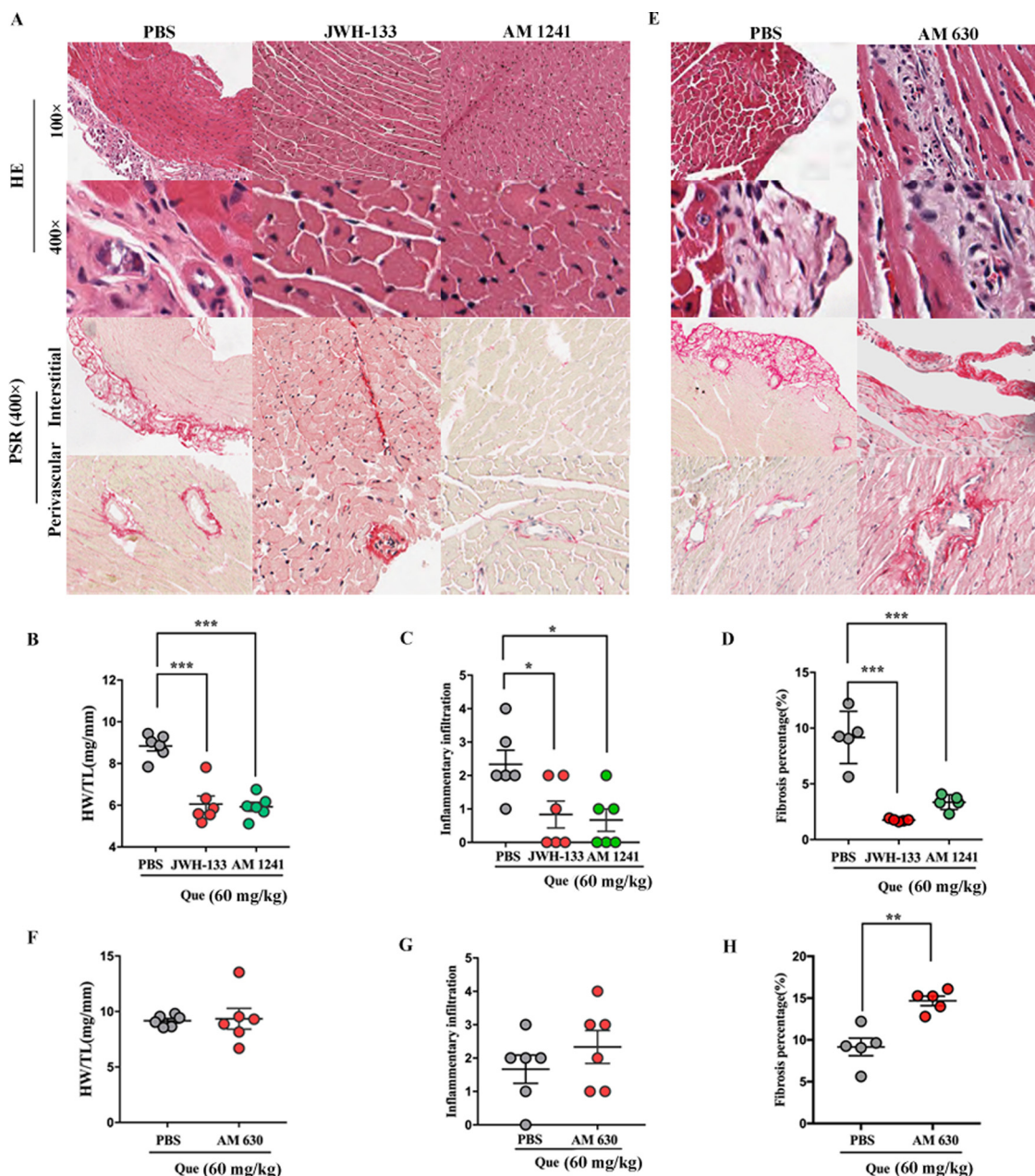


**Fig. 7.** Pharmacologic activation of CB2R protected against Que cardiotoxicity. (A) In a first experimental set, mice were pretreated with PBS, CB2R agonists JWH-133 or AM 1241 (n = 6 mice/group) before the start of Que insult. Twenty-one days after treatments, mice were sacrificed. Heart sections were stained with HE and PSR reagents for histological examination. Activation of CB2R by either agonist remarkably relieved the myocardium toxicity. (B) Effects of CB2R agonists on the HW/TL ratio. (C, D) CB2R agonists induced sheer decreases in the myocardium inflammation index and percentage of fibrosis. (E) In a second experiment, mice were pretreated with PBS or a specific CB2R antagonist AM 630 (n = 6 mice/group) 1 h before injection of Que. Heart sections were stained with HE or PSR reagents for histological examination. Blockade of CB2R worsened Que toxic effect as evidenced by HE and PSR staining in morphology. (F) The HW/TL was calculated for PBS or AM 630-pretreated mice. (G, H) Effects of AM 630 (CB2R antagonist) on the inflammatory infiltration and fibrosis in PBS or AM 630-pretreated mice. HE staining, hematoxylin and eosin staining. PSR, PicroSirius Red. HW/TL, heart weight/tibia length. \*,  $p < 0.05$ , \*\*,  $p < 0.01$ , \*\*\*,  $p < 0.001$  as indicated.

**3.8. CBRs agents regulated the activation process of necroptosis**

In view of the observations that Que specifically induced necroptotic cell deaths and pharmacologic modulation of CBRs exerted protective roles in Que cardiotoxicity, we then assessed whether CBRs regulated the cell necroptosis process. Initially, we detected the effects of CBR agent alone on necroptosis. In the Que-free cells, single treatment of JWH-133 (1μM), AM 1241 (5μM), AM 281 (2μM), or Rimo (2μM) caused no remarkable effect on necroptosis by western blot analysis (Fig. 8A). Under the insult of Que, both CB1R antagonists and CB2R agonists consistently decreased the protein levels of MLKL and

inhibited the phosphorylation of MLKL (p-MLKL) (Fig. 8B). Moreover, CB1R antagonists were more effective than CB2R agonists in the myocardial cells with respect to the protein levels of RIP1 and RIP3 (Fig. 8B). Furthermore, the translocation of MLKL was visualized through immunofluorescence assay and it was shown that either assessed agent (JWH-133, AM 1241, AM 281 or Rimo) restored MLKL plasma location which greatly contradicted to Que-exposed cells that presented with evident MLKL membrane location (Fig. 8C). Multiplexed IHC analysis also found that Que alone caused MLKL translocation to cell membrane (black arrow) with both RIP3 (pink signal) and MLKL (brown signal) elevation. The pretreatment of either above CBR agent

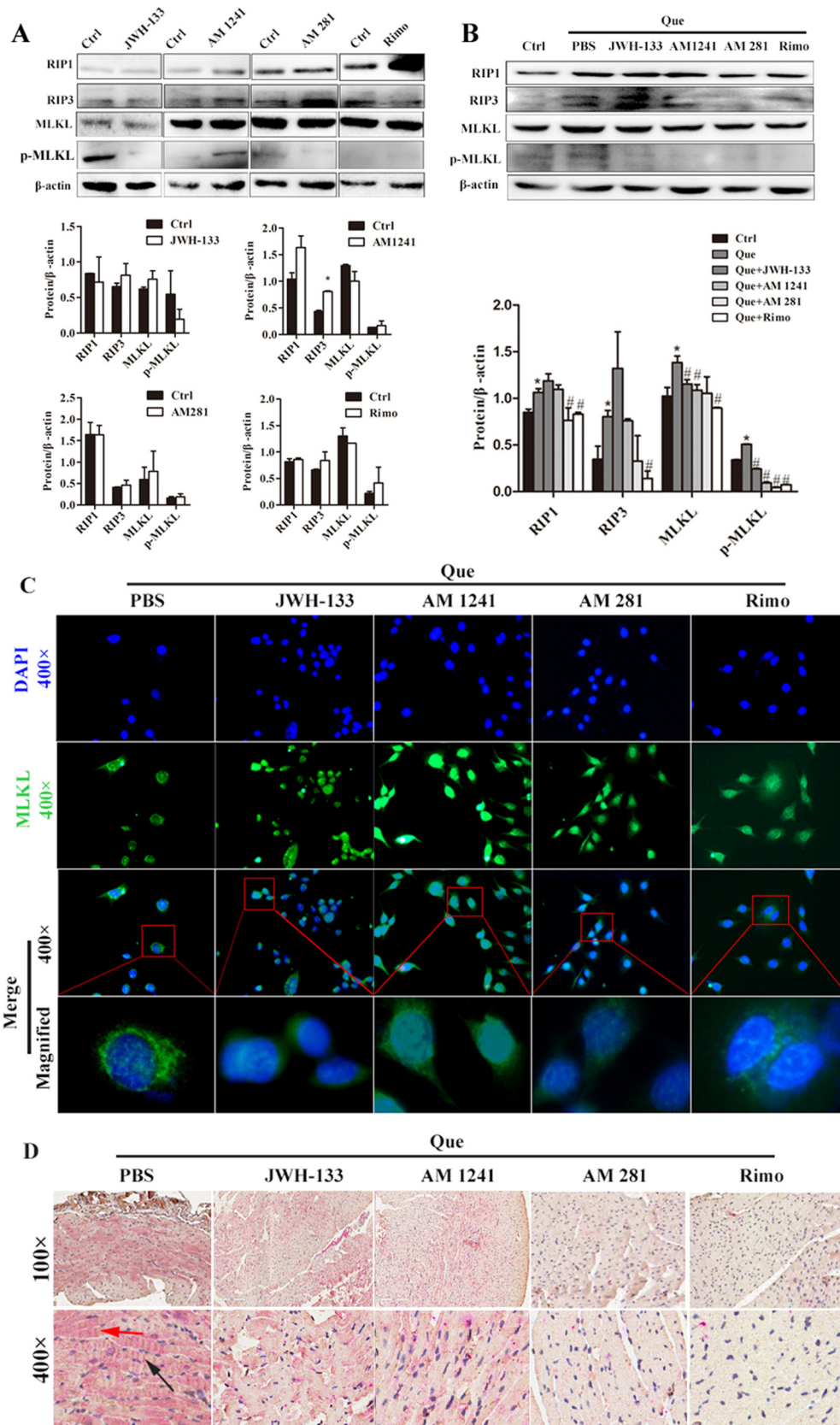


**Fig. 8.** The beneficial agents of CBRs suppressed cell necroptosis process. (A, B) The assessed protective agents (CB1R antagonists and CB2R agonists) were pretreated to Que-free (A) or Que (2μM)-insulted HL-1 cells (B) for 24 h. After 24 h, western blot analysis was performed to detect the necroptosis (upper panels). The intensity was quantified using ImageJ (lower panels). (C) Immunofluorescence assay showed that either CB1R antagonists or CB2R agonists blocked the cytomembrane localization of MLKL induced by Que (2μM). (D) Multiplexed IHC analysis of the necroptosis markers RIP3 (pink) and MLKL (brown) in heart slides from indicated groups. Black arrow indicates the brown signal (MLKL) in membrane and red arrow indicates the RIP3 signal. CBR, cannabinoid receptor; Rimo, Rimonabant. \*,  $p < 0.05$  vs. Ctrl. #,  $p < 0.05$  vs. Que.

(JWH-133, AM 1241, AM 281 or Rimo) blunted the MLKL elevation and stabilized the plasma location of MLKL (Fig. 8D). All these data suggested that the beneficial agents of CBRs suppressed Que-induced cell necroptosis process.

#### 4. Discussion

Quetiapine serves as an atypical antipsychotic drug due to its property of effective pharmacologic functions, but in recent years it has

attracted clinician's attention and wary prescription due to its side effect particularly towards myocardium (Coffey and Williams, 2011; Melada et al., 2016; Perlis, 2007). Similar with other antipsychotics, Que-induced cardiotoxicity is clinically manifested as prolongation of the QTc interval, tachycardia, and even sudden cardiac death (Papazisis et al., 2012; Wassef et al., 2015). Pathologically, drug-induced myocardial injury is non-specific and presents with inflammation infiltration and/or fibrosis accumulation, termed as myocarditis and cardiomyopathy in the disease state. The present study used a clinical comparable dose of Que for continuous injection into mice to establish a murine model of Que cardiotoxicity. Compared with placebo-treated group, Que exposure caused remarkable inflammatory cells accumulation and the aggravation of fibrotic lesions surrounding vessels and in the myocardial interstitium as evidenced by the HE staining and PSR staining. With the exposure hours extended or doses concentrated, Que significantly impaired cardiomyocyte viability. Quetiapine-exposed cells showed necrotic-like morphologic changes under electron microscope. All these experimental evidence confirmed Que-induced cardiac toxicity *in vivo* and *in vitro*.

The fundamental impact of drug toxicity is to cause death of cells (Linkermann and Green, 2014). The Que-treated cardiomyocytes showed disrupted membrane integrity, mitochondria swelling and reticulum expansion, all of which are indicators of necrotic cell death. Therefore, the currently defined types of cell death were detected, including cell apoptosis, autophagy and necroptosis which are programmed and signal through defined pathway. As the results showed, Que induced activation of major mediators of cell necroptosis but with inconsistent effects on other proteins involved in apoptosis and autophagy. Que activated cardiomyocyte necroptosis most stably as compared with Clz and Olz, another two atypical antipsychotics. Since necroptosis has been documented to involve in multiple drug toxicity and pharmacologic inhibition of it conferred protection against drug toxic effects (Linkermann and Green, 2014; Xu et al., 2018; Yuan and Kaplowitz, 2013), the specific inhibitor Nec-1 was used *in vivo*. Nec-1 pretreatments indeed inhibited the necroptosis process. Nec-1 significantly attenuated heart edema and pathological remodeling as measured by the HW/TL ratio and significantly suppressed Que-induced fibrotic lesions ( $p < 0.01$ ). These data confirmed the therapeutic potential of Nec-1 in cardiovascular diseases (Gupta et al., 2018).

It is worth noting that Nec-1 pretreatments failed to rescue the inflammatory cell aggravation after Que insult. This might be explained by drawbacks regarding the clinical applicability of Nec-1. Nec-1 was the first compound to be identified as an inhibitor of necroptosis by allosterically targeting RIP1 (Degterev et al., 2008). However, metabolic stability of Nec-1 is very limited ( $T_{1/2} < 5$  min in mouse microsomal assay) (Degterev et al., 2013; Teng et al., 2005). Nec-1 was later pointed out to have off-target activity and identified to also inhibit indoleamine 2, 3-dioxygenase (IDO, also known as IDO1), which is an enzyme involved in tryptophan metabolism (Takahashi et al., 2012). In this setting, optimized Nec-1 analogues such as 7-Cl-O-Nec-1 would represent a superior tool over Nec-1 due to its  $T_{1/2} \sim 1$  h in liver microsomal assay and its exclusive selectivity towards RIP1 (Degterev et al., 2013; Teng et al., 2005).

Alternatively, identification of the upstream regulators of cellular necroptosis would aid in providing novel pharmacologic target for drug development. As a large family of cell-surface receptors, G protein-coupled receptors have received wide attention and over 30% of current commercial drugs are developed by targeting G protein-coupled receptors (Drews, 2000). Cannabinoid receptors belong to the superfamily of G protein-coupled receptors and have been implicated as attractive therapeutic approach for cardiovascular diseases (Martin et al., 2018). In a previous study, we have reported that two subtypes of CBRs (CB1R and CB2R) were critically involved and had conflicting roles in Clz-induced myocardial injury (Li et al., 2019). Herein, we also detected that the major endocannabinoids (AEA and 2-AG) decreased their levels upon Que insult. CB1R internalized, while CB2R kept at the

cell surface after Que insult, indicating an opposite manner by which CBRs transduced extracellular signal. Pharmacologic inhibition of CB1R or the selective activation of CB2R conferred strong protection against Que toxicity, which were evidenced by the relieved inflammation infiltration and fibrotic lesions in hearts. In particular, the CB1R antagonists (Rimo, AM 281) or the agonists of CB2R (JWH-133, AM 1241) inhibited the necroptosis activation processes following Que treatments. These data were conclusive that CBRs were the upstream regulators of necroptosis. CBRs mediated Que-induced cardiac toxicity by regulating necroptosis process.

Interestingly, either CB1R antagonists or CB2R agonists significantly dampened the HW/TL ratio, cardiac inflammation index and fibrosis extent, three indicators for heart dysfunction. In comparison, Nec-1, the inhibitor of necroptosis, only showed marginal inhibition of infiltration index. Very short half-life of Nec-1 might be one explanation (Weinlich et al., 2017). A larger group size may also aid in justifying the efficacy of Nec-1. An additional interpretation would be that beneficial CBRs agents are superior over RIP1-targeted small-molecule inhibitors with regard to the therapeutic efficacy. Pharmacological inhibitors of necroptosis have evolved and improved versions of Nec-1 have been developed with longer half-life or higher specificity (Weinlich et al., 2017). Unfortunately, neither inhibitor has been confirmed to be in perfect clinical application. Pharmacological modulators of CBRs, however, have obtained great progress into clinical application. Though Rimo has been withdrawn due to its high propensity to induce psychiatric adverse effects such as major depressive episodes (Sherafat-Kazemzadeh et al., 2013), the identification of CB1R antagonists/CB2R agonists serves us a unique view that pharmacologic targeting of CBRs could confer beneficial effects during drug cardiotoxicity. Therefore, the potential advantages of CBR antagonists/agonists merit further investigation and open novel therapeutic clues for drug development.

Of note, the present study revealed an opposite effect of CB1R and CB2R in Que cardiotoxicity, that is, CB1R antagonists or CB2R agonists were cardioprotective. It reminded advisors that it would not benefit from dual antagonist or dual agonist of CBRs since dual binding might neutralize the effect of each other. Therapeutics should be mono-receptor based.

## 5. Conclusion

The present study established the first Que-induced cardiotoxicity *in vivo* and *in vitro* and based on the experimental models; it was found that Que promoted the necroptotic cell death to induce cardiac toxicity. Selective CB1R antagonists or the selective CB2R agonists provide beneficial potentials against Que-induced cardiotoxicity.

## Declaration of Competing Interest

The authors declare that they have no known competing financial interests or personal relationships that could have appeared to influence the work reported in this paper.

## Transparency document

The Transparency document associated with this article can be found in the online version.

## Acknowledgements

This work was financially supported by the National Natural Science Foundation of China (grant No.: 81701861 and 81871525), China Postdoctoral Science Foundation (grant No.: 2016M601507 and 2018T110348), Zhengyi Scholar Foundation of School of Basic Medical Sciences, Fudan University (grant No.: s22-10) and the Opening Project of Shanghai Key Laboratory of Crime Scene Evidence (grant No.: 2018XCWZK22).

## References

- Adameova, A., Hrdlicka, J., Szobi, A., Farkasova, V., Kopaskova, K., Murarikova, M., Neckar, J., Kolar, F., Ravingerova, T., Dhalla, N.S., 2017. Evidence of necroptosis in hearts subjected to various forms of ischemic insults. *Can. J. Physiol. Pharmacol.* 95, 1163–1169.
- Cai, Z., Jitkaew, S., Zhao, J., Chiang, H.C., Choksi, S., Liu, J., Ward, Y., Wu, L.G., Liu, Z.G., 2014. Plasma membrane translocation of trimerized MLKL protein is required for TNF-induced necroptosis. *Nat. Cell Biol.* 16, 55–65.
- Coffey, S., Williams, M., 2011. Quetiapine-associated cardiomyopathy. *N. Z. Med. J.* 124, 105–107.
- Coulter, D.M., Bate, A., Meyboom, R.H., Lindquist, M., Edwards, I.R., 2001. Antipsychotic drugs and heart muscle disorder in international pharmacovigilance: data mining study. *BMJ* 322, 1207–1209.
- Degterev, A., Hitomi, J., Gersmeyer, M., Ch'En, I.L., Korkina, O., Teng, X., Abbott, D., Cuny, G.D., Yuan, C., Wagner, G., Hedrick, S.M., Gerber, S.A., Lugovskoy, A., Yuan, J., 2008. Identification of RIP1 kinase as a specific cellular target of necrostatins. *Nat. Chem. Biol.* 4, 313–321.
- Degterev, A., Maki, J.L., Yuan, J., 2013. Activity and specificity of necrostatin-1, small-molecule inhibitor of RIP1 kinase. *Cell Death Differ.* 20, 366.
- Dong, X., Li, L., Ye, Y., Zhang, D., Zheng, L., Jiang, Y., Shen, M., 2018. Surrogate analyte-based quantification of main endocannabinoids in whole blood using liquid chromatography-tandem mass spectrometry. *Biomed. Chromatogr.* e4439.
- Drews, J., 2000. Drug discovery: a historical perspective. *Science* 287, 1960–1964.
- du Plessis, S.S., Agarwal, A., Syriac, A., 2015. Marijuana, phytocannabinoids, the endocannabinoid system, and male fertility. *J. Assist. Reprod. Genet.* 32, 1575–1588.
- Fernandez-Ruiz, J., Romero, J., Ramos, J.A., 2015. Endocannabinoids and neurodegenerative disorders: Parkinson's disease, Huntington's chorea, Alzheimer's disease, and others. *Handb. Exp. Pharmacol.* 231, 233–259.
- Gerra, G., Zaimovic, A., Gerra, M.L., Ciccocioppo, R., Cippitelli, A., Serpelloni, G., Somaini, L., 2010. Pharmacology and toxicology of Cannabis derivatives and endocannabinoid agonists. *Recent Pat. CNS Drug Discov.* 5, 46–52.
- Gong, Y.N., Guy, C., Crawford, J.C., Green, D.R., 2017. Biological events and molecular signaling following MLKL activation during necroptosis. *Cell Cycle* 16, 1748–1760.
- Gupta, K., Phan, N., Wang, Q., Liu, B., 2018. Necroptosis in cardiovascular disease - a new therapeutic target. *J. Mol. Cell. Cardiol.* 118, 26–35.
- Huang, R., Liu, W., 2015. Identifying an essential role of nuclear LC3 for autophagy. *Autophagy* 11, 852–853.
- Jakobsen, K.D., Wallach-Kildemoes, H., Bruhn, C.H., Hashemi, N., Pagsberg, A.K., Fink-Jensen, A., Nielsen, J., 2017. Adverse events in children and adolescents treated with quetiapine: an analysis of adverse drug reaction reports from the Danish Medicines Agency database. *Int. Clin. Psychopharmacol.* 32, 103–106.
- Lee, S.H., Kim, H.R., Han, R.X., Oqani, R.K., Jin, D.I., 2013. Cardiovascular risk assessment of atypical antipsychotic drugs in a zebrafish model. *J. Appl. Toxicol.* 33, 466–470.
- Li, L., Dong, X., Tu, C., Li, X., Peng, Z., Zhou, Y., Zhang, D., Jiang, J., Burke, A., Zhao, Z., Jin, L., Jiang, Y., 2019. Opposite effects of cannabinoid CB1 and CB2 receptors on antipsychotic clozapine-induced cardiotoxicity. *Br. J. Pharmacol.* 176 (7), 890–905.
- Li, L., Ye, X., Zhao, Z., Gao, P., Jiang, Y., 2018. Overlooked fatal infectious diseases after long-term antipsychotic use in patients with psychiatric illness. *Schizophr. Res.* 195, 258–259.
- Linkermann, A., Green, D.R., 2014. Necroptosis. *N. Engl. J. Med.* 370, 455–465.
- Martin, G.V., Noriega, S.E., Kassuha, D.E., Fuentes, L.B., Manucha, W., 2018. Anandamide and endocannabinoid system: an attractive therapeutic approach for cardiovascular disease. *Ther. Adv. Cardiovasc. Dis.* 12, 177–190.
- Melada, A., Krcmar, T., Vidovic, A., 2016. A dose-dependent relationship between quetiapine and QTc interval. *Int. J. Cardiol.* 222, 893–894.
- Papazisis, G., Mastrogianni, O., Chatziniolaou, F., Vasiliadis, N., Raikos, N., 2012. Sudden cardiac death due to quetiapine overdose. *Psychiatry Clin. Neurosci.* 66, 535.
- Perlis, R.H., 2007. Treatment of bipolar disorder: the evolving role of atypical antipsychotics. *Am. J. Manag. Care* 13, S178–S188.
- Pertwee, R.G., 2015. Endocannabinoids and their pharmacological actions. *Handb. Exp. Pharmacol.* 231, 1–37.
- Roesch-Ely, D., Van Einsiedel, R., Kathofer, S., Schwaninger, M., Weisbrod, M., 2002. Myocarditis with quetiapine. *Am. J. Psychiatry* 159, 1607–1608.
- Romao, S., Munz, C., 2014. LC3-associated phagocytosis. *Autophagy* 10, 526–528.
- Salvo, F., Pariente, A., Shakir, S., Robinson, P., Arnaud, M., Thomas, S., Raschi, E., Fourrier-Regat, A., Moore, N., Sturkenboom, M., Hazell, O.B.O.I., 2016. Sudden cardiac and sudden unexpected death related to antipsychotics: a meta-analysis of observational studies. *Clin. Pharmacol. Ther.* 99, 306–314.
- Sherafat-Kazemzadeh, R., Yanovski, S.Z., Yanovski, J.A., 2013. Pharmacotherapy for childhood obesity: present and future prospects. *Int. J. Obes. (Lond.)* 37, 1–15.
- Stack, E.C., Wang, C., Roman, K.A., Hoyt, C.C., 2014. Multiplexed immunohistochemistry, imaging, and quantitation: a review, with an assessment of Tyramide signal amplification, multispectral imaging and multiplex analysis. *Methods* 70, 46–58.
- Szobi, A., Rajtik, T., Adameova, A., 2016. Effects of necrostatin-1, an inhibitor of necroptosis, and its inactive analogue Nec-1i on basal cardiovascular function. *Physiol. Res.* 65, 861–865.
- Takahashi, N., Duprez, L., Grootjans, S., Cauwels, A., Nerinckx, W., DuHadaway, J.B., Goossens, V., Roelandt, R., Van Hauwermeiren, F., Libert, C., Declercq, W., Callewaert, N., Prendergast, G.C., Degterev, A., Yuan, J., Vandenebee, P., 2012. Necrostatin-1 analogues: critical issues on the specificity, activity and in vivo use in experimental disease models. *Cell Death Dis.* 3, e437.
- Teng, X., Degterev, A., Jagtap, P., Xing, X., Choi, S., Denu, R., Yuan, J., Cuny, G.D., 2005. Structure-activity relationship study of novel necroptosis inhibitors. *Bioorg. Med. Chem. Lett.* 15, 5039–5044.
- Traynor, K., 2009. FDA advisers wary of expanding quetiapine use: clinicians air concerns about metabolic effects, tardive dyskinesia. *Am. J. Health. Syst. Pharm.* 66 (880), 882.
- Vieweg, W.V., 2003. New generation antipsychotic drugs and QTc interval prolongation. *Prim. Care Companion J. Clin. Psychiatry* 5, 205–215.
- Wassef, N., Khan, N., Munir, S., 2015. Quetiapine-induced myocarditis presenting as acute STEMI. *BMJ Case Rep.* 2015.
- Weinlich, R., Oberst, A., Beere, H.M., Green, D.R., 2017. Necroptosis in development, inflammation and disease. *Nat. Rev. Mol. Cell Biol.* 18, 127–136.
- Wu, C.S., Tsai, Y.T., Tsai, H.J., 2015. Antipsychotic drugs and the risk of ventricular arrhythmia and/or sudden cardiac death: a nation-wide case-crossover study. *J. Am. Heart Assoc.* 4.
- Xie, X., Zhao, Y., Ma, C.Y., Xu, X.M., Zhang, Y.Q., Wang, C.G., Jin, J., Shen, X., Gao, J.L., Li, N., Sun, Z.J., Dong, D.L., 2015. Dimethyl fumarate induces necroptosis in colon cancer cells through GSH depletion/ROS increase/MAPKs activation pathway. *Br. J. Pharmacol.* 172, 3929–3943.
- Xu, Z., Jin, Y., Yan, H., Gao, Z., Xu, B., Yang, B., He, Q., Shi, Q., Luo, P., 2018. High-mobility group box 1 protein-mediated necroptosis contributes to dasatinib-induced cardiotoxicity. *Toxicol. Lett.* 296, 39–47.
- Yuan, L., Kaplowitz, N., 2013. Mechanisms of drug-induced liver injury. *Clin. Liver Dis.* 17, 507–518.
- Zhou, F., Jiang, X., Teng, L., Yang, J., Ding, J., He, C., 2018. Necroptosis may be a novel mechanism for cardiomyocyte death in acute myocarditis. *Mol. Cell. Biochem.* 442, 11–18.